

Supporting Information

Substituent Effect on Controlled Release of Fragrant Aldehydes from pH-triggered Nicotinoylhydrazone-based Precursors

Zoubing Xiao^{a, b}, Chengjing Wu^a, Xinyu Lu^{a*}, Yunwei Niu^a, Peiran Yu^a, and Xiaojie Ma^a

a. School of Perfume and Aroma Technology, Shanghai Institute of Technology, Shanghai 201418, China

b. School of Agriculture and Biology, Shanghai Jiao Tong University, Shanghai 200240, China

Contents

1. Weight loss and odor of the four fragrance precursors	S2
2. Infrared information of four fragrance precursors.....	S2
3. ¹ H, ¹³ C NMR and Mass spectra of four fragrance precursors.....	S2–S6
4. Changes of uv absorption curves of four fragrance precursors in pH 2 and pH 6 standard buffer solutions	S7
5. Aroma compounds release concentration of four fragrance precursors in pH2, pH6 standard buffer solutions.....	S7
6. Release kinetic models of four fragrance precursors in pH2, pH6 standard buffers solutions.....	S8
7. Results of the Kirby Bauer test for the agar medium placed over the layer of NTA2 and control.....	S8

1. Weight loss and odor of the four fragrance precursors

Table S1. Weight loss and odor of the four fragrance precursors.

fragrance precursors	weight /mg (under atmosphere, 25°C, RH 30%)			odor (pure water as reference)	
	initial	after one year	weight loss (%)	in water ($c = 35.0 \mu\text{molL}^{-1}$)	solid
NTA1	1538.3	1537.7	0.039	odorless	odorless
NTA2	1497.2	1496.8	0.027	odorless	odorless
NTA3	1500.6	1499.9	0.047	odorless	odorless
NTA4	1489.4	1489.1	0.020	odorless	odorless

2. Infrared information of four fragrance precursors

Table S2. Effect of electronic properties and positions of substitution groups on the IR spectra of fragrance precursors (potassium bromide, cm^{-1}).

fragrance precursors	FT-IR (cm^{-1})					
	VNH	VC=O	VC=N	VPh-O-Me	VPh-iPr	VPh-OH
NTA1	3486	1695	1596			
NTA2	3463	1688	1570	1168		
NTA3	3278	1681	1565		2972	
NTA4	3287	1686	1552			1295

3. ^1H , ^{13}C NMR and Mass spectra of four fragrance precursors

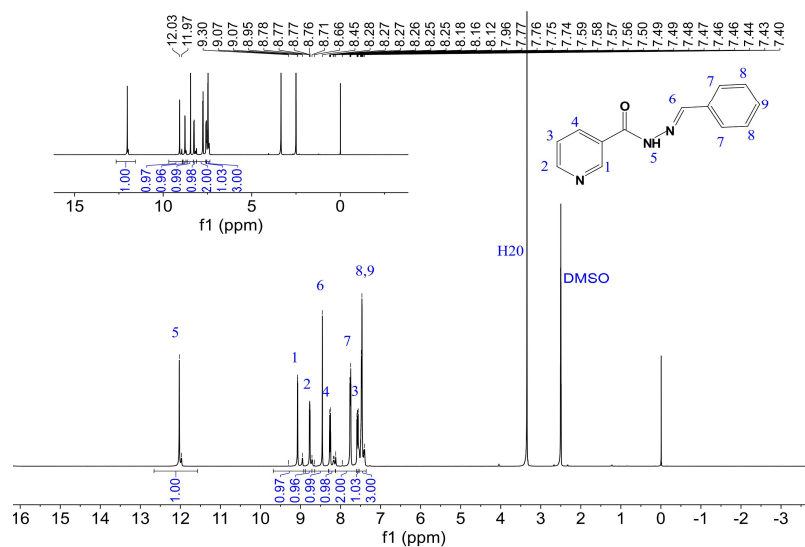


Figure S1. ^1H NMR spectrum of compound NTA1 in DMSO.

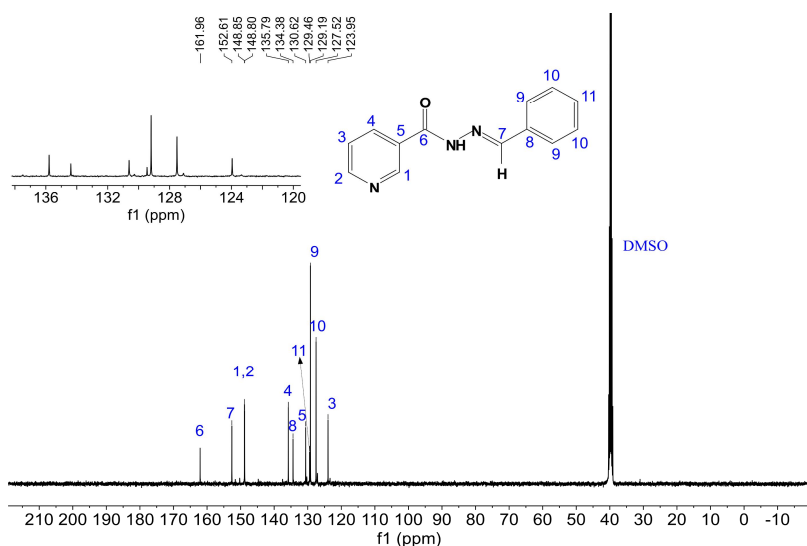


Figure S2. ^{13}C NMR spectrum of compound NTA1 in DMSO.

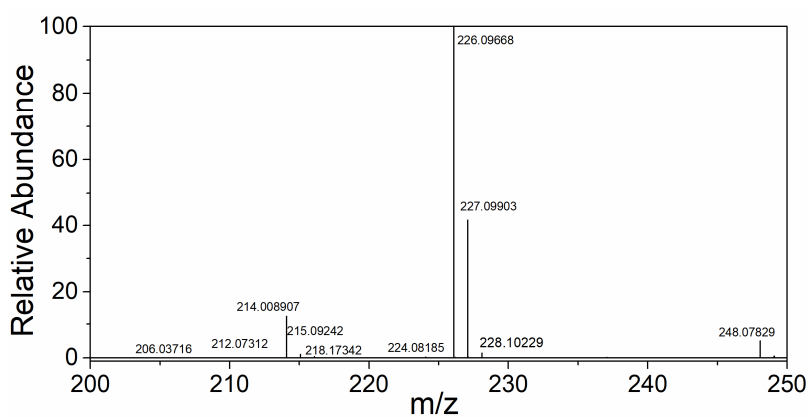


Figure S3. HRMS spectrum of compound NTA1.

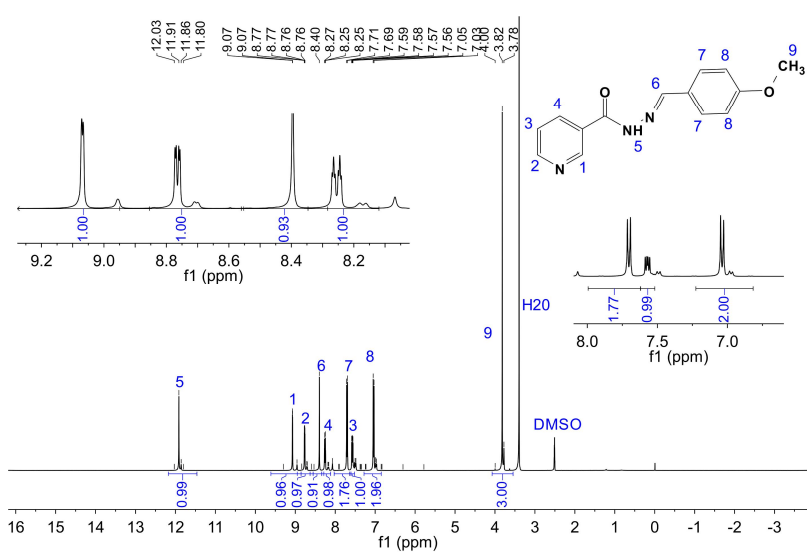


Figure S4. ^1H NMR spectrum of compound NTA2 in DMSO.

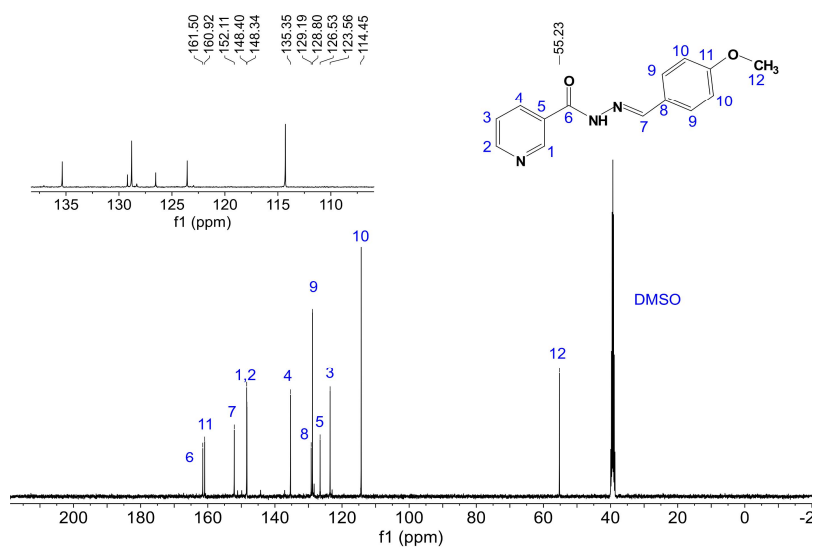


Figure S5. ^{13}C NMR spectrum of compound NTA2 in DMSO.

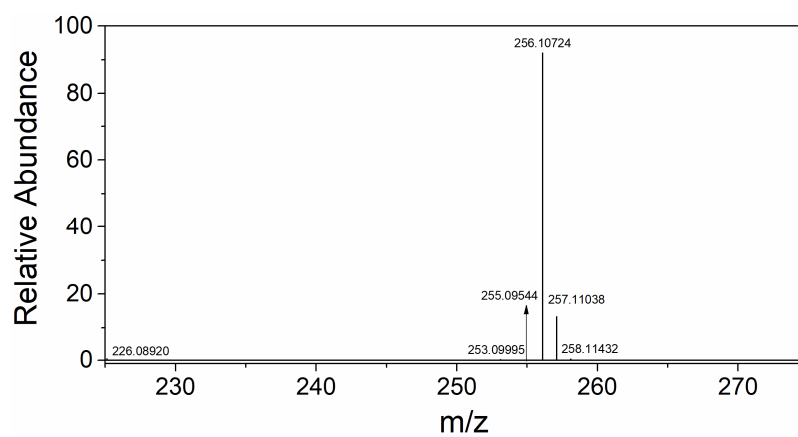


Figure S6. HRMS spectrum of compound NTA2.

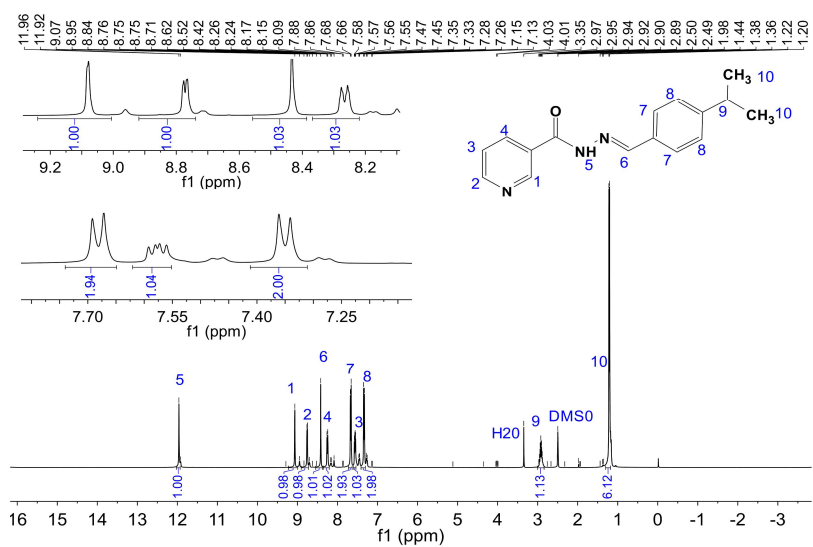


Figure S7. ^1H NMR spectrum of compound NTA3 in DMSO.

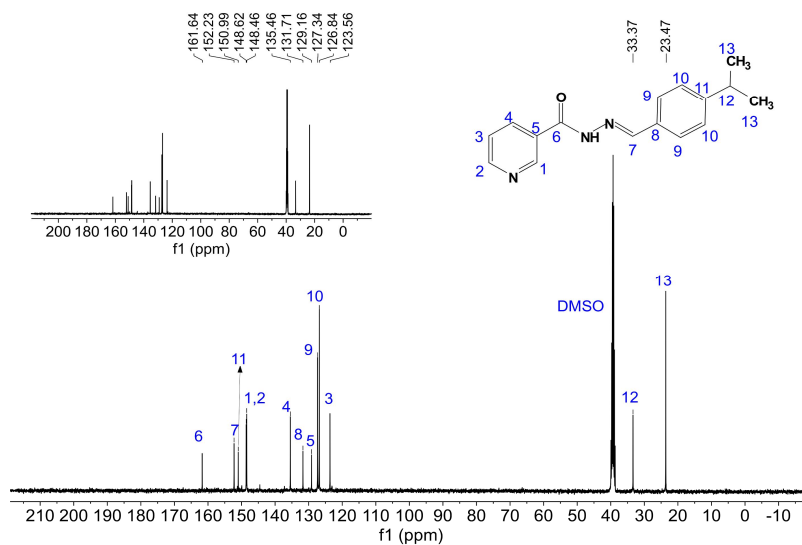


Figure S8. ¹³C NMR spectrum of compound NTA3 in DMSO.

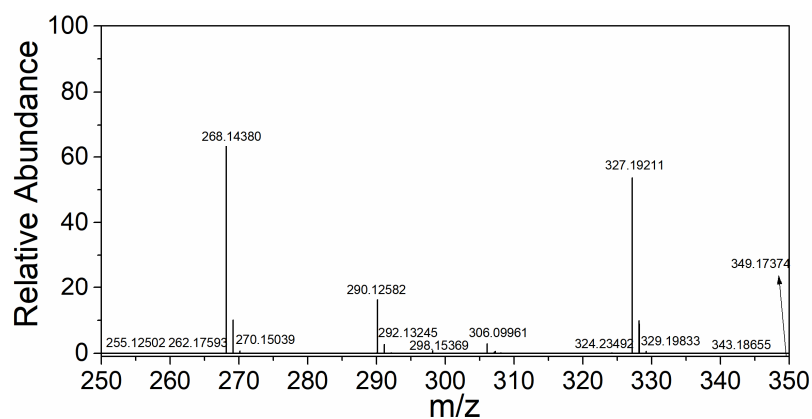


Figure S9. HRMS spectrum of compound NTA3.

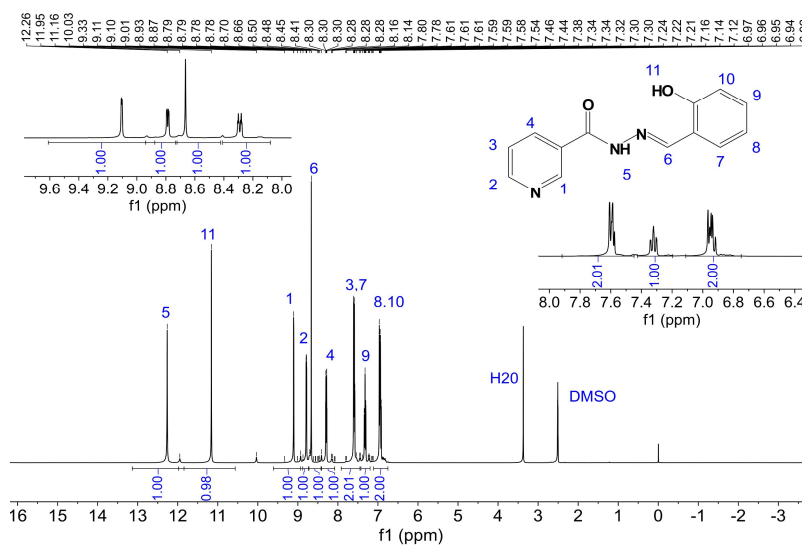


Figure S10. ¹H NMR spectrum of compound NTA4 in DMSO.

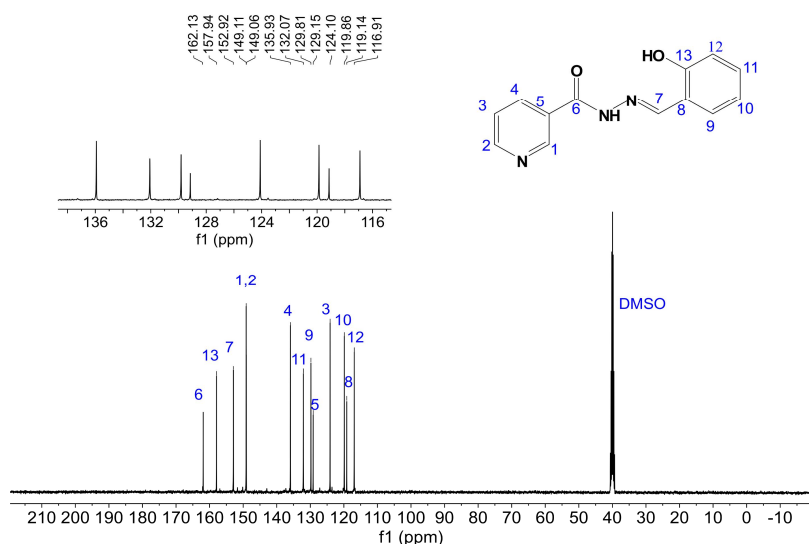


Figure S11. ¹³C NMR spectrum of compound NTA4 in DMSO.

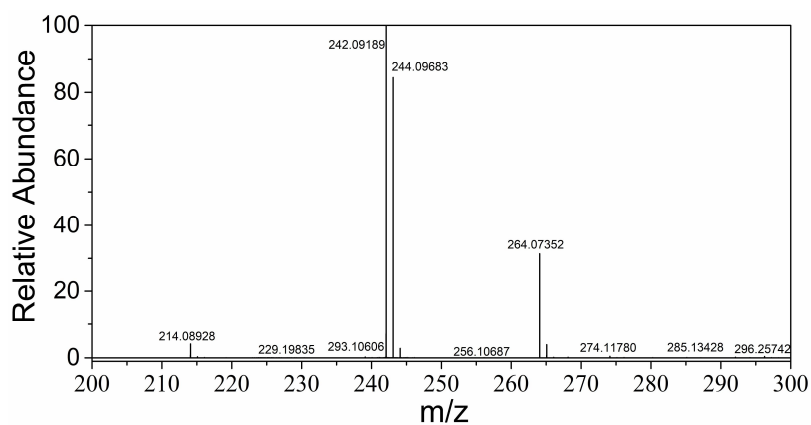


Figure S12. HRMS spectrum of compound NTA4.

Table S3. HRMS spectrum of compound data of compound NTA1-NTA4.

Fragrance precursor	Calculated	Found
NTA1	226.0975	226.0967
NTA2	256.1080	256.1072
NTA3	268.1444	268.144
NTA4	242.0240	242.0919

4. Changes of uv absorption curves of four fragrance precursors in pH 2 and pH 6 standard buffer solutions

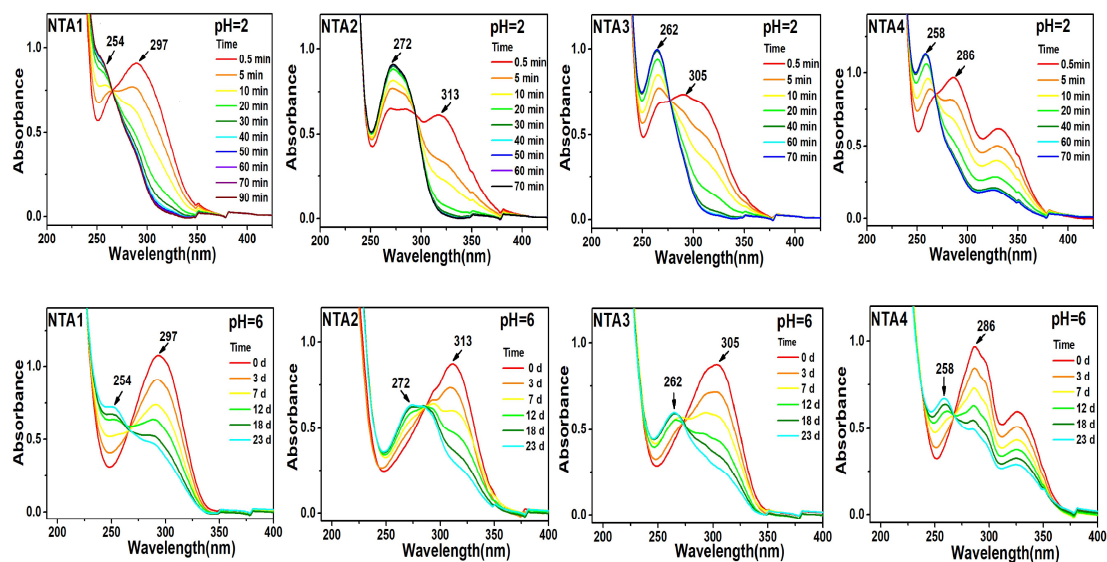


Figure S13. Time-dependent UV-Vis absorbance of NTA1-NTA4 in buffer solution (pH 2.0, 6.0).

5. Aroma compounds release concentration of four fragrance precursors in pH2, pH6 standard buffer solution

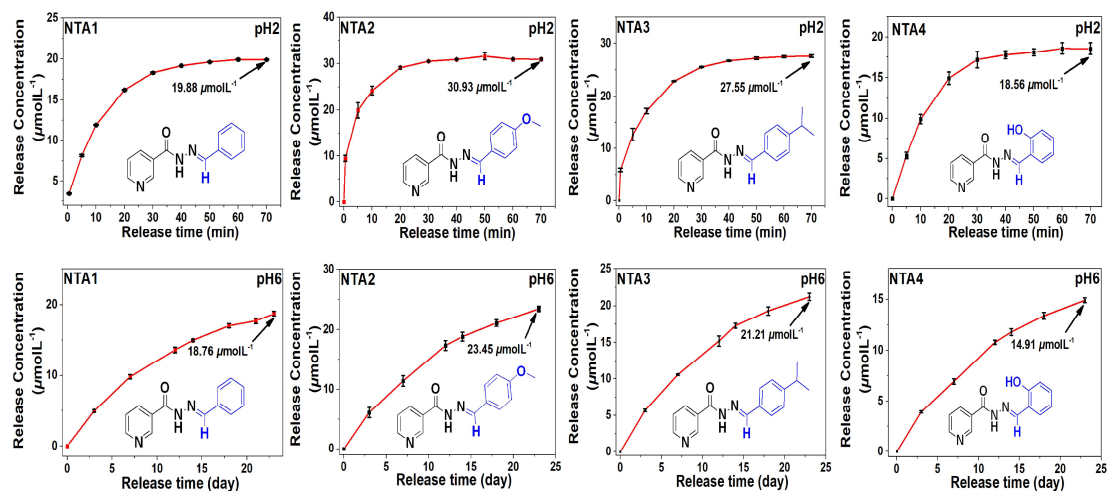


Figure S14. Time-dependent release concentration of NTA1-NTA4 in buffer solution (pH 2.0, 6.0).

6. Release kinetic models of four fragrance precursors in pH 2, pH 6 standard buffers solutions

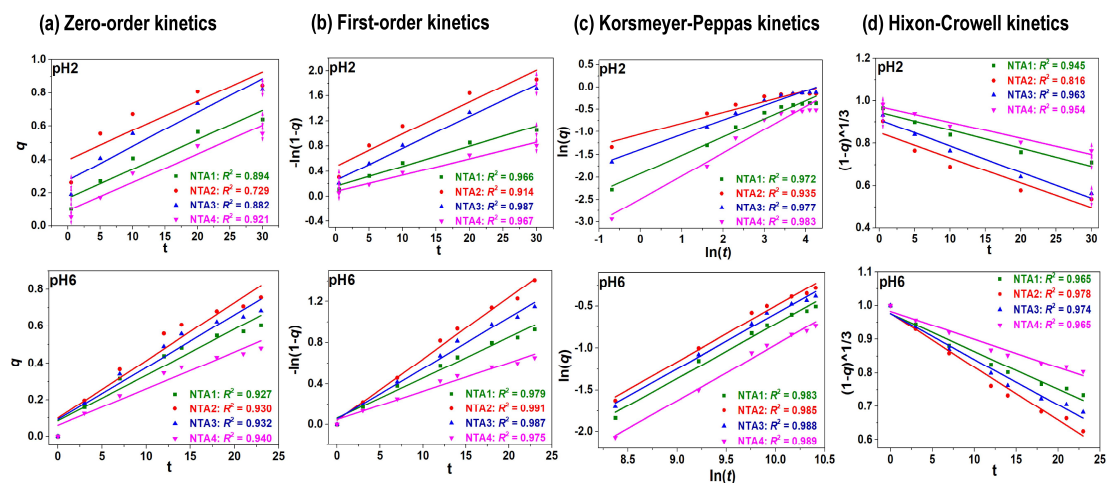


Figure S15. Kinetic models and the corresponding best-fit constants of fragrance precursors NTA1–NTA4 in buffer solution (pH 2.0, 6.0)

7. Results of the Kirby Bauer test for the agar medium placed over the layer of NTA2 and control.

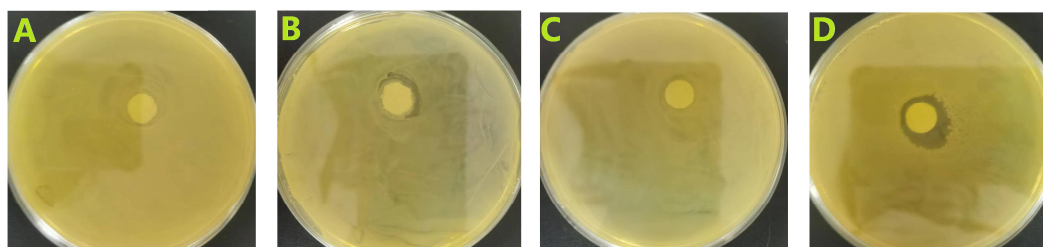


Figure S16. Results of the Kirby Bauer test of *Staphylococcus aureus* (A: control, B: NTA2), and *Escherichia coli* (C: control, D: NTA2).